Available online at www.sciencedirect.com
SCIENCE DIRECT®
ELSEVIER
Nuclear Instruments and Methods in Physics Research B 200 (2003) 295–302
NIM B
Beam Interactions with Materials & Atoms
www.elsevier.com/locate/nimb

X-ray tomographic imaging of Al/SiC_p functionally graded composites fabricated by centrifugal casting

A. Velhinho [a,b,*], P.D. Sequeira [c], Rui Martins [a], G. Vignoles [d], F. Braz Fernandes [a,b], J.D. Botas [b], L.A. Rocha [c,e]

[a] *CENIMAT – Centro de Investigação em Materiais, Faculdade de Ciências e Tecnologia, Universidade Nova de Lisboa, Quinta da Torre, Caparica 2829-516, Portugal*

[b] *DCM – Departamento de Ciência dos Materiais, Faculdade de Ciências e Tecnologia, Universidade Nova de Lisboa, Quinta da Torre, Caparica 2829-516, Portugal*

[c] *CIICS – Centro de Investigação em Comportamento de Superficies, Universidade do Minho, Campus de Azurém, 4800-058 Guimarães, Portugal*

[d] *LCTS – Laboratoire des Composites Thermostructuraux, Université de Bordeaux 1 – Domaine Universitaire – 3, Allée La Boetie – F 33600 Pessac, France*

[e] *DEM – Departamento de Engenharia Mecânica, Escola de Engenharia, Universidade do Minho, Campus de Azurém, 4800-058 Guimarães, Portugal*

Abstract

The present work refers to an X-ray microtomography experiment aiming at the elucidation of some aspects regarding particle distribution in SiC-particle-reinforced functionally graded aluminium composites.

Precursor composites were produced by rheocasting. These were then molten and centrifugally cast to obtain the functionally graded composites. From these, cylindrical samples, around 1 mm in diameter, were extracted, which were then irradiated with a X-ray beam produced at the European Synchrotron Radiation Facility.

The 3-D images were obtained in edge-detection mode. A segmentation procedure has been adapted in order to separate the pores and SiC particles from the Al matrix. Preliminary results on the particle and pore distributions are presented.

PACS: 81.05.Ni; 42.30.Wb; 07.05.Pj

Keywords: X-ray microtomography; Metal-matrix composites; Functionally graded materials; Centrifugal casting; Rheocasting; Image processing

1. Introduction

A prime motivation for research in the area of aluminium-based metal matrix composites (MMC's) stems from the interest of the automotive industry in producing cast engine blocks and other automobile components – cylinder liners,

* Corresponding author. Address: Departamento de Ciência dos Materiais, Faculdade de Ciências e Tecnologia, Universidade Nova de Lisboa, Quinta da Torre, Caparica 2829-516, Portugal. Tel.: +351-25-351-02-20/+351-21-294-85-64; fax: +351-25-351-60-07/+351-21-295-78-10.

E-mail addresses: ajv@fct.unl.pt, ajv@engmateriais.eng.uminho.pt (A. Velhinho).

0168-583X/02/$ - see front matter
PII: S0168-583X(02)01691-9

pistons and valves, among other examples – using this type of material. Many potential benefits of MMC's over conventional iron-based alloys derive from a combination of important weight savings with the attractive tribological properties of the MMC's surface. However, a low to moderate toughness of conventional MMC's is disadvantageous to some applications, with a simultaneous requirement for high wear resistance and high bulk toughness, so as to allow the component to absorb impact loads [1]. Functionally graded Al–Si composites selectively reinforced at the surface by SiC particles are a promising response to this problem.

Knowledge about the spatial distribution of the reinforcement, which is of significant importance in the case of conventional MMC's, becomes paramount in the case of ceramic particle-reinforced functionally graded materials (FGM's), namely due to its implication in failure processes [2].

Centrifugal casting is one of the most effective methods for processing SiC-particle-reinforced Al-based FGM's. In this case, spatial distribution of the particles depends upon the momentum imparted to each individual particle by the centrifugal force, on the collisions between ceramic particles, as well as upon the interactions between the ceramic particles and the metallic matrix (wetting ability, particle segregation due to a moving solidification front). However, accurate control of the distribution of the particles and of the mechanisms leading to their distribution is not well understood [3]. The situation is further complicated if one considers the presence of voids and pores within the material. Porosity can have different causes (gas dissolved by the matrix or adsorbed at the surface of the particles, inadequate liquid feeding during casting, solidification shrinkage) and may as a result exhibit differing morphologies, but it will invariably contribute to microstructural inhomogeneity and affect the particle distribution.

Although conventional techniques based on 2-D metallographic image analysis are quite capable of estimating important parameters, namely particle size distribution [4,5] and particle volume fraction [4–10], some 3-D stereological parameters, namely interparticle connectivity [11], are beyond its reach. Such parameters can only be assessed directly by techniques where the three-dimensional nature is an intrinsic characteristic, as is the case with tomography. Moreover, the features under evaluation, by their scale, demand spatial resolutions in the order of 10 μm or less, thus leading to the use of X-ray microtomography with synchrotron radiation.

The classical form of X-ray microtomography, based on X-ray attenuation, can permit a resolution near 1 μm, depending on the radiation used and on the sample and material characteristics [12]. However, in the case of Al/SiC composites, because the constituents exhibit very similar attenuation coefficients, the contrast obtained is unsatisfactory, placing serious reconstruction difficulties.

An alternative type of X-ray microtomography has recently been developed [12,13]. It exploits the differences in phase which are generated due to two parallel rays passing on each size of an interface between two constituents of the material. A compromise is thus reached, where a small loss in spatial resolution is compensated by a much-enhanced contrast between the constituents.

However, even if phase contrast allows the immediate production of understandable images, these are not suited to subsequent computations, since they do not consist of density fields and normally do not exhibit uninterrupted borders between reinforcement and matrix. These questions were recently addressed in a work by Vignoles [14], where a segmentation procedure was developed and successfully applied to the case of C/C composites.

In the present paper, the same algorithm is applied to a Al/SiC_p functionally graded composite, in order to investigate the distribution of the reinforcements and how these interact with the porosity present in the material. For this particular case, the procedure had to be adapted in order to identify separately the pores and the SiC inclusions.

2. Materials and methods

2.1. Composite production

2.1.1. Rheocasting of precursor composites

A capacity for the production of functionally graded SiC_p-reinforced aluminium-matrix

composites exists at Universidade do Minho. However, due to limitations in the configuration of the centrifugal casting apparatus, it becomes necessary to work from precursor composites, whether commercially available or produced in the laboratory. Thus, a precursor composite was rheocast from commercial Al–7Si–0.3Mg ingot material, which was reinforced by SiC particles. A Coulter LS230 laser interpherometer was used to determine size distribution of the SiC particles added to the melt. Average grain size of SiC particles was 37.5 μm.

To produce rheocast composites, the alloy is molten and subsequently cooled under controlled conditions to the chosen temperature within the semi-solid domain, where it is maintained for a pre-determined time, in order to develop a non-dendritic morphology in the matrix and to promote dispersion of the ceramic reinforcement particles added. In order to achieve these goals, the slurry is stirred by an impeller. At the same time, the slurry is protected from oxidation by the injection of a N_2 current in the crucible. The material is then poured into a metallic mould and, while in the semi-solid state, is compressed in order to reduce the amount of porosity induced by the stirring action, being subsequently water quenched. The apparatus and related technique are described in detail elsewhere [15–17]. The processing conditions for the rheocast precursor composites are summarized in Table 1. The particle content of the precursor composite was evaluated through density measurements, in accordance with Chawla [18].

Table 1
Processing conditions of the composites used in the present study

Rheocasting conditions	
Stirring speed (rpm)	600
Stirring temperature (°C)	610
Stirring time (prior to SiC addition) (min)	30
Stirring time (after SiC addition) (min)	40
Primary solid vol. fraction (vol.%)	10
SiC volume fraction (vol.%)	10
Centrifugal casting conditions	
Pouring temperature (°C)	750
Mould temperature (°C)	20
Time taken to achieve maximum angular acceleration (s)	9

The composites were produced from an Al–7Si–0.3Mg alloy and SiC particles with 37.5 μm mean size.

2.1.2. Centrifugal casting of functionally graded composites

To produce the FGM composite, ≈0.2 kg of the precursor composite were melted and centrifuged using a *Titancast 700 μP Vac* furnace, from *Linn High Therm*, Germany. This furnace, illustrated in Fig. 1, possesses a vacuum chamber (vacuum pressure: $P < 0.3$ Pa) located in the extremity of a rotating arm moving around a vertical axis. Inside the chamber there is space to mount a vertically positioned alumina crucible containing the precursor composite, centred within an induction-heating coil, as well as a horizontal graphite mould material, equipped with a dedicated resistance-heating system. The vacuum chamber allows the passage of a series of K-type thermocouples, used to monitor the melt temperature, as well as the mould and FGM temperatures.

When the melt reaches the desired temperature, the induction coil is lowered and a torque corresponding to a pre-selected program is applied to the rotating arm, thus imposing the desired acceleration pattern to the ensemble. The resulting angular velocity is measured by a system working with eddy-currents induced in a detector by a magnet fixed in the rotating arm. During rotation, which lasts for 90 s, the melt is forced from the crucible, and is conducted through a pouring hole into the mould, where it cools down and solidifies. The samples produced are cylindrical in shape, with 40 mm both in length and diameter.

The processing conditions for the centrifugally cast FGM composite can be found in Table 1.

2.2. X-ray microtomography

Samples from the FGM were analysed by X-ray microtomography at the ID 19 beamline of the European Synchrotron Radiation Facility, in Grenoble.

Those samples, cylindrical in shape and around 1 mm in diameter, were machined by EDM with their axis parallel to the direction of the functional gradient. The original positions of the samples defined a regular grid.

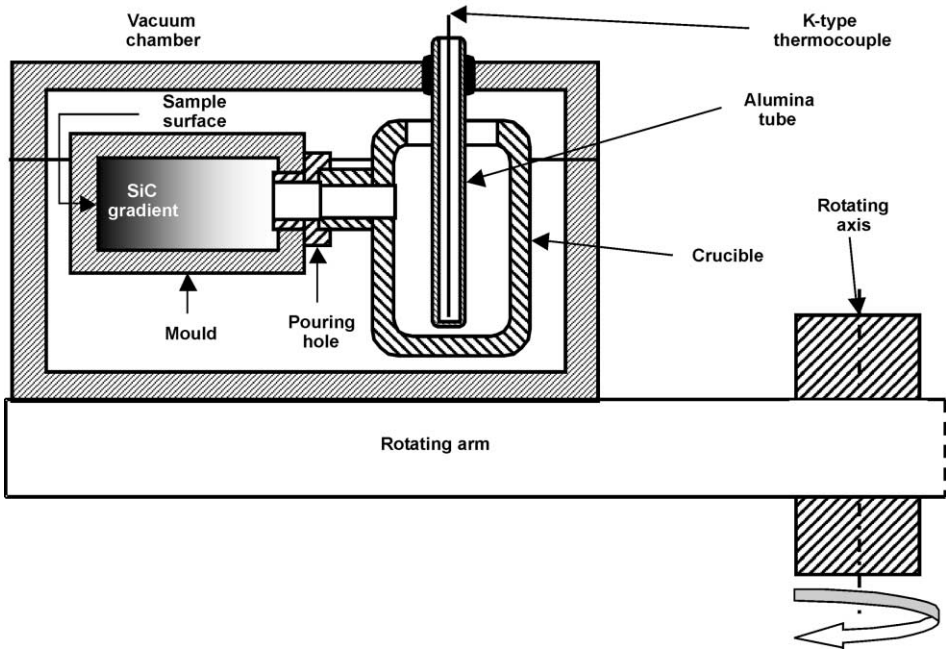

Fig. 1. Schematic representation of the casting arm of the furnace. The region of segregated SiC particles is indicated in the scheme. This region is referred to in the text as ''surface''.

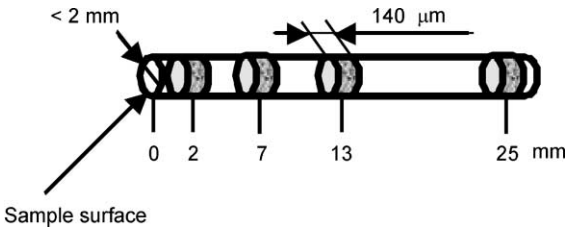

Fig. 2. Schematic representation of the functionally graded composite samples studied in the experiment. Each sample was obtained by EDM machining of a centrifugally cast composite. From each, several tomographs were recorded, corresponding to ROI at 2, 7, 13 and 25 mm from the SiC-rich surface.

From each sample several regions of interest (ROI) were scanned, as illustrated in Fig. 2. In total, 9 samples, summing up to 36 ROI, were analysed during the course of the experiment. Given the resolution obtained in the experimental conditions available at ID 19, each of these ROI results in a substantial dataset. For this reason, in the present work our attention will focus exclusively on a single representative sample, extracted close to the longitudinal axis of the FGM composite. Subsequent data processing has been carried out on subsets of these ROI's, which will henceforward be designated as volume of interest (VOI).

The microtomography measurements were performed using a beam energy of 20 keV, employing a multilayer as monochromator. The sample was placed at 100 mm from the detector, a FRELON 1024×1024 CCD camera. This distance gave access to edge-detection mode in order to enhance contrast between SiC particles and aluminium matrix. Pixel size was 0.95 μm.

2.3. Image segmentation procedure

Because X-ray absorption contrast between the matrix and the reinforcing particles was still too weak to allow easy image segmentation, the resulting datasets required further treatment, with the use of a modified version of the algorithm developed at LCTS [14].

The principle of this procedure is: (1) a classification by double thresholding of the pixels in three

regions: black, grey, and white. Black and white pixels carry the information of the nature of the phase. (2) One or two hysteresis steps are necessary in order to ensure that all black/white patterns fully enclose the remaining objects, and (3) every connected subset of grey pixels is painted according to the mean colour of its envelope.

In this case, where three phases are present, the first step was to identify the pores, characterized by a very strong phase contrast. Then, once the pores were segmented, they were dilated twice, in order to create a mask corresponding to the pores plus their phase contrast patterns, which was then deduced from the original image. Finally, the procedure was repeated in order to separate the inclusions.

3. Results and discussion

In Fig. 3 a SEM micrograph is presented in which the shape of SiC reinforcing particles is shown. As it can be seen, particles present sharp edges and a relatively wide range of shapes, ranging from spheroid-like to platelet-like. As determined from laser interpherometry measurements, particle grain size ranges from ≈20 to 70 μm, with a median size of 37.5 μm.

Previous works [4,5,7,8,19] have shown the value of hardness profiles as a good indication of the particle volume fraction gradient within the FGM composite. Thus, this technique was employed to perform a preliminary characterization of the material produced. Results obtained show that the maximum hardness value occurs at some distance from the FGM surface. Previous works have shown that this variation in properties can be controlled during processing, by playing with the balance between the velocity of SiC particles advancing towards the surface under the influence of centrifugal force, and the solidification front which moves in the opposite direction, hindering the movement of the reinforcements [4,5].

X-ray microtomography images obtained in the FGM composite were subjected to the segmentation procedure described above, which permitted the reconstruction of the various VOIs.

3.1. Particle analysis

In Fig. 4 a histogram showing the particle size distribution in the VOI (1.73 mm^3) located at 13 mm from the surface is presented. The first remark is the presence of a bimodal distribution (modes located at ≈20 and ≈35 μm). This situation should be compared with the grain size distribution of the particles that were used to fabricate the composite (unimodal distribution). The second maximum observed in Fig. 4 is likely to correspond to the distribution of SiC particles in the volume under

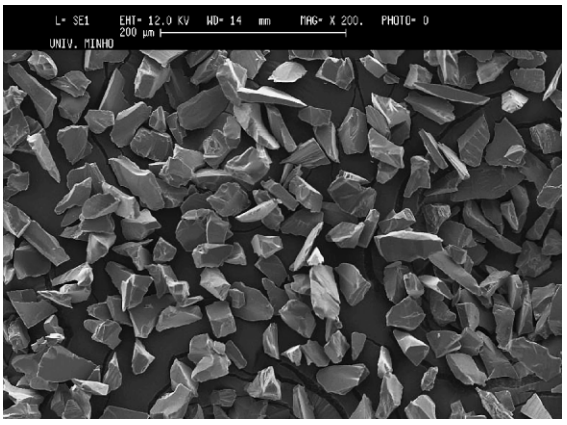

Fig. 3. SEM imaging of the SiC particles employed as reinforcing-agent in the composites produced. The sharp-edged shape of the particles is particularly noteworthy.

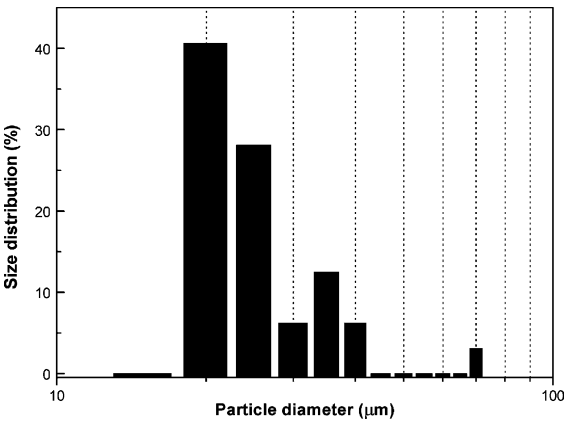

Fig. 4. Particle size distribution in the VOI situated at 13 mm from the surface of the sample, as determined after reconstruction of microtomographic data.

analysis. Previous work [5] has shown that particle segregation along the axis of the composite caused by centrifugal casting can occur to some extent. It means that the mean particle diameter profile measured as a function of the depth below the surface of the cast FGM may vary from point to point.

Nevertheless, the maximum located at ≈20 μm observed in Fig. 6 also suggests that the present results are strongly affected by the presence of artefacts in the image. In fact, during both the fabrication of the precursor composite and the centrifugal casting processing, forces acting in the particles are not strong enough to lead to significant particle fragmentation [5]. However, as referred before, X-ray absorption contrast between the matrix and the reinforcing particles is very weak. Also, ring artefacts and streaks are present in the original dataset. Although, a dedicated image segmentation procedure was developed to analyse such images, further improvements regarding the filtering of the data is needed to remove noise which induces the ''presence'' of a very high number of low dimension particles.

In Fig. 5 the ratio of bounding box volume to reconstructed particle volume is plotted. The bounding box is defined as a parallelepiped whose edge length is the same as the measured maximum sizes of the particle along the three axes of the reconstructed block. As a consequence the graph can be used to assess the shape of the particles. As it can be seen most particles are far from having a spherical shape. The same conclusion can be drawn from the reconstructed image presented in Fig. 6, and is in good agreement with the SEM micrograph shown in Fig. 3. Therefore, the computation involved in the processing of data presented in Fig. 4, where the SiC particles were approximated by spheres, may also be affected by more or less significant deviations.

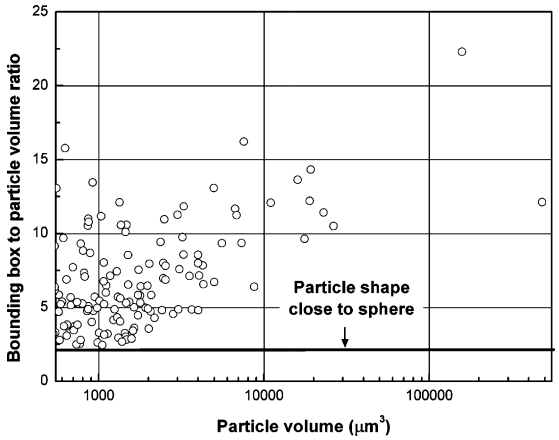

Fig. 5. Particle shape characterization in the VOI situated at 13 mm from the surface of the sample, showing that the majority of the particles exhibit shapes far from that of a sphere.

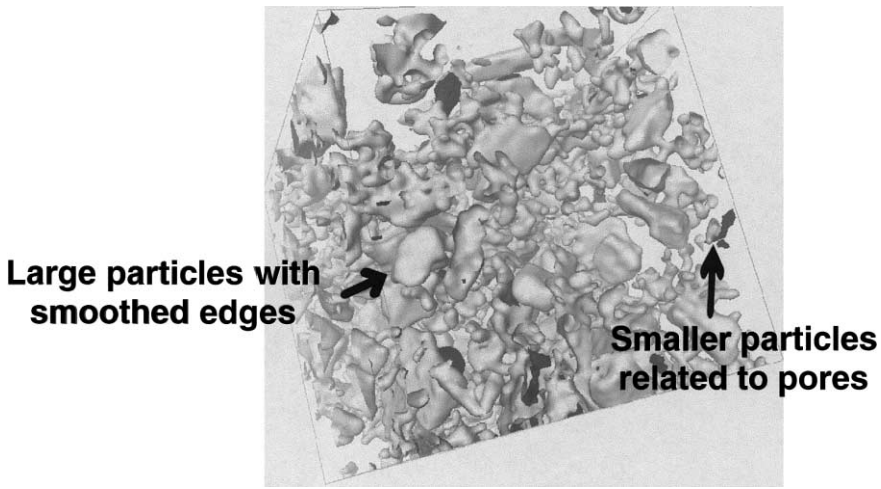

Fig. 6. Simultaneous 3-D rendering of pores and particles in a sample located at 13 mm from the top. Sample size: 200^3 voxels $\Longleftrightarrow 0.19^3$ mm^3.

Comparing the shape of the particles in the reconstructed images (see Fig. 6) to that obtained by SEM (Fig. 3), it should be remarked that the reconstructed particles exhibit much smoother edges. This results from the segmentation algorithm, which cannot capture curvature radii lower than 1 or 2 pixels.

The reconstructed volume also shows, apart from the reinforcing particles, the presence of a number of pores. Indeed, some of the particles appear to be grouped together in large clusters, frequently in association with pores. This probably results from wetting problems during elaboration.

3.2. Porosity analysis

In Fig. 7 pore shape characterization in the VOI located at 13 mm from the sample surface is presented. The plot shows the existence of at least two different types of porosity: one corresponding to spherical pores, and the other to non-spherical pores or pore clusters. As shown in the graph spherical pores generally present dimensions below $\approx 60\ \mu m^3$. Spherical pores are usually attributed to the presence of small amounts of gas dissolved in the matrix during casting, and can be found isolated within the aluminium matrix. The reconstructed image presented in Fig. 6, also shows that a complex shape pore network, i.e. non-spherical

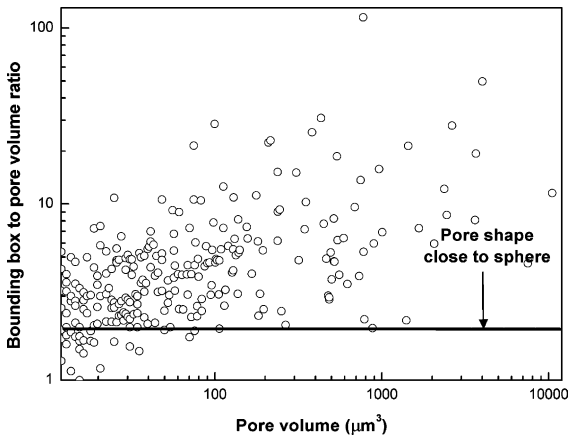

Fig. 7. Pore shape characterization in the VOI situated at 13 mm from the surface of the sample, evidencing two different kinds of pores: smaller spherical pores (ratio $\cong 2$) and aspherical pores of varying dimensions.

Table 2
Porosity and particle volume fraction distribution

Distance from surface (mm)	Porosity volume fraction (%)	Particle volume fraction (%)
2	1.3	17.7
7	2.0	17.4
13	0.8	16.0

pores, is present in close relation to ceramic particles clusters, probably denoting wetting problems during elaboration.

3.3. Gradient analysis

Despite the limitations of the segmentation procedure already mentioned, it was possible to estimate the extent of the gradients obtained by centrifugal casting. Therefore, porosity and SiC particle fraction have been measured at three different locations in the sample (2, 7 and 13 mm from the surface). The results are summarized in Table 2. The particle fraction displays a monotonous decrease from the surface to the interior of the sample. This behaviour is consistent with the hardness measurements performed (as previously mentioned in Section 3), and indicates the presence of a gradient of the particle distribution along the sample.

Regarding porosity, results suggest that a higher amount exists near the sample surface. This is probably due to the higher particle density existing at the surface. In fact, as referred above, owing to wetting problems, a complex pore network is associated with ceramic particle clusters.

4. Conclusions

Image segmentation of X-ray microtomography data allows 3-D qualitative information about pore and particle distributions to be obtained. It could be observed that as a consequence of centrifugal casting SiC particles are partially clustered, with some pores gathered with them, this being associated to imperfect wetting of ceramic particles by the molten aluminium alloy. Also, small spherical pores, associated to trapped gas

bubbles, are observed dispersed in the matrix. In addition, it was possible to quantify the particle volume fraction profile along the centrifugally cast FGM composite. Results show a relatively smooth gradient of ceramic particles along the sample, which can be beneficial in terms of mechanical performance of the material. Nevertheless, refinements of the image segmentation procedure are still needed in order to filter noise introduced by image artefacts.

Acknowledgements

The authors wish to acknowledge E. Boller and P. Cloetens, as well as all the remaining staff at ESRF, for their assistance and cooperation during the microtomography experiments.

The financial support obtained by A. Velhinho from Fundo Social Europeu, under the program PRODEP, is gratefully acknowledged. Part of the work was supported by Fundação para a Ciência e Tecnologia (FCT – Portugal), under contract POCTI/12301/2001.

References

[1] M.R. Jolly, The Foundryman 5 (November) (1990) 509.
[2] T.W. Clyne, P.W. Withers, in: E.A. Davis, I.M. Ward (Eds.), An Introduction to Metal Matrix Composites, CUP, Cambridge, 1993, p. 510.
[3] Y. Watanabe, N. Yamanaka, Y. Fukui, Compos. Part A 29A (1998) 595.
[4] L.A. Rocha, A.E. Dias, D. Soares, C.M. Sá, A.C. Ferro, Ceram. Trans. 114 (2001) 467.
[5] L.A. Rocha, P.D. Sequeira, A. Velhinho, C.M. Sá, in: XVI Congresso Brasileiro de Engenharia Mecânica, 2001, p. 381.
[6] L. Lajoye, M. Suéry, in: Proceedings of International Symposium on Advances in Cast Reinforced Metal Composites, ASM International, 1988, p. 15.
[7] Y. Watanabe, Y. Fukui, Recent Res. Dev. Metall. Mater. Sci. 4 (2000) 51.
[8] Y. Watanabe, Y. Fukui, Aluminum Trans. 2 (2000) 195.
[9] A. Ourdjini, K.C. Chew, B.T. Hhoo, J. Mat. Proc. Technol. 116 (2001) 72.
[10] R. Rodríguez-Castro, R.C. Wetherhold, M.H. Kelestemur, Mater. Sci. Eng. A 323 (2002) 445.
[11] J.-M. Chaix, Journées d'Automne 2001 de la Société Française de Métallurgie et de Matériaux, Paris, 2001, p. 80.
[12] E. Maire, J.-Y. Buffière, L. Salvo, J.J. Blandin, W. Ludwig, J.M. Létang, Adv. Eng. Mater. 3 (2001) 539.
[13] J.-Y. Buffière, E. Maire, P. Cloetens, G. Lormand, R. Fougères, Acta Mater. 47 (1999) 1613.
[14] G. Vignoles, Carbon 39 (2001) 167.
[15] C. Ferreira, J. Teixeira, J.D. Botas, in: Proc. 8° Encontro da Soc. Portuguesa de Materiais, 1997, p. 9.
[16] C. Ferreira, Processos Tecnológicos Associados è Reo-Fundição, Ph.D. Thesis, Universidade Nova de Lisboa, 1999, p. 305.
[17] A. Velhinho, F.M. Braz Fernandes, J.D. Botas, Key Engineering Materials 2001, in: 1st International Materials Symposium, Coimbra, 2001; Mater. Sci. Forum 230–232 (2002) 226.
[18] K. Chawla, Composite Materials Science and Engineering, first ed., Verlag, 1987, p. 177.
[19] Y. Watanabe, N. Yamanaka, Y. Oya-Seimiya, Y. Fukui, Z. Metallkd. 92 (2001) 53.